

Utah State University

DigitalCommons@USU

Space Dynamics Lab Publications

Space Dynamics Lab

1-1-1993

Cryogenic Infrared Radiance Instrumentation for Shuttle (CIRRIS 1A) Instrumentation and Flight Performance

Brent Bartschi
Utah State University

Allan Steed

Jeffery Blakeley

Follow this and additional works at: https://digitalcommons.usu.edu/sdl_pubs

Recommended Citation

Bartschi, Brent; Steed, Allan; and Blakeley, Jeffery, "Cryogenic Infrared Radiance Instrumentation for Shuttle (CIRRIS 1A) Instrumentation and Flight Performance" (1993). *Space Dynamics Lab Publications*. Paper 11.

https://digitalcommons.usu.edu/sdl_pubs/11

This Article is brought to you for free and open access by the Space Dynamics Lab at DigitalCommons@USU. It has been accepted for inclusion in Space Dynamics Lab Publications by an authorized administrator of DigitalCommons@USU. For more information, please contact digitalcommons@usu.edu.



Cryogenic infrared radiance instrumentation for shuttle (CIRRIS 1A)
instrumentation and flight performance

Brent Bartschi, Allan Steed, Jeffery Blakeley

Space Dynamics Laboratory
Utah State University, Logan, UT 84322-4140

Mark Ahmadjian, Jack Griffin, Richard Nadile

Geophysics Directorate of the USAF Phillips Laboratory
Hanscom Air Force Base, MA 01731

ABSTRACT

The Cryogenic Infrared Radiance Instrumentation for Shuttle (CIRRIS 1A) instrument, launched on the shuttle Discovery (STS-39) on 28 April 1991, was developed to characterize the phenomenology and dynamics of ionospheric processes. The primary objective of the CIRRIS 1A mission was to obtain spectral and spatial measurements of infrared atmospheric emissions in the spectral region between 2.5 and 25 μm over altitudes ranging from the Earth's surface to 260 km. The primary sensors are a Michelson interferometer/spectrometer and a multi-spectral radiometer, which share a common high off-axis rejection telescope. The sensor/telescope complex is enclosed in a cryogenic dewar that is mounted in a dual-axis gimbal system. Excellent data were obtained from this mission, and preliminary analysis shows that all sensors performed well. This paper describes the experiment hardware, summarizes instrument performance during flight, and presents examples of significant results.

1. INTRODUCTION

The Geophysics Directorate of the United States Air Force Phillips Laboratory participates in upper atmospheric and space-related research programs to meet its space-defense program requirements of establishing an extensive, detailed atmospheric infrared emission information base. This research requires characterizing background conditions, including emissions produced by atomic and molecular species in the Earth's upper atmosphere, along with target signatures. The Cryogenic Infrared Radiance Instrumentation for Shuttle (CIRRIS 1A) program was developed to collect this information.

CIRRIS 1A is a state-of-the-art, cryogenically cooled instrument designed to observe the infrared spectrum of the Earth's atmosphere. The instrument was designed, constructed, calibrated, and tested by the Space Dynamics Laboratory at Utah State University (SDL/USU), and features two primary infrared sensors: a high-resolution Michelson interferometer and a high-spatial-resolution radiometer. Both sensors share the collection optics of a single telescope complex. The sensor/telescope complex is enclosed in a cryogenic dewar, and the dewar is mounted in a two-axis gimbal. Affixed to the outside of the dewar are two photometers with integrated sun sensors, two low-light-level television cameras, a film camera celestial aspect sensor, and a horizon sensor.

CIRRIS 1A, designated as AFP-675 on the National Space Transportation System manifest, was launched on the shuttle Discovery on 28 April 1991 and resulted in a very successful mission, with nearly 100% of the mission goals achieved. The primary goal of the CIRRIS 1A experiment was to collect simultaneous high resolution spectral and spatial measurements in the 2.5 to 25 μm region, from altitudes ranging from the Earth's surface to 260 km, over a range of latitudes, day/night conditions, and geomagnetic activity. The main observation targets were earthlimb airglow, celestial targets, and auroral emissions. Data obtained from this experiment will help refine knowledge of the background radiance and structure of atmospheric infrared emissions, and will be used to update and validate U.S. Air Force atmospheric models, which are used in the design of operational systems. This paper describes the CIRRIS 1A mission objectives and experiment hardware, summarizes instrument performance during flight, and presents examples of significant flight data results.

2. MISSION OBJECTIVES

The primary objective of the CIRRIS 1A mission was to obtain simultaneous spectral and spatial measurements of atmospheric emissions in the 2.5-25 μm infrared region over an altitude ranging from the Earth's surface to 260 km. Secondary objectives were to measure targets of opportunity (TOOs), such as low-Earth-orbit satellites passing within viewing range of the sensor.

Figure 1 shows the most current U.S. Air Force radiance model of atmospheric airlimb emissions for the infrared region between 2 and 26 μm at a tangent height of 100 km. This figure shows significant emission peaks at 5.3 μm (NO), 10 μm (O_3), and 15 μm (CO_2). Superimposed on this trace is the emission plot of a cold satellite target; clearly, the airlimb emissions overwhelm the satellite emissions, except in narrow areas or "windows" between strong atmospheric bands. An infrared sensor, in order to detect a satellite or similar target, must thus be filtered to admit radiation only from the narrow window areas. The goal of the CIRRIS 1A experiment was to precisely define the extent of the spectral windows, including:

- 1) optimum wavelengths of atmospheric windows for detecting cold body targets
- 2) background radiance levels in these window regions
- 3) spatial structure (clutter) of the background in terms of power spectral densities (PSDs)
- 4) variabilities of earthlimb emissions as a function of day/night and geomagnetic activity.

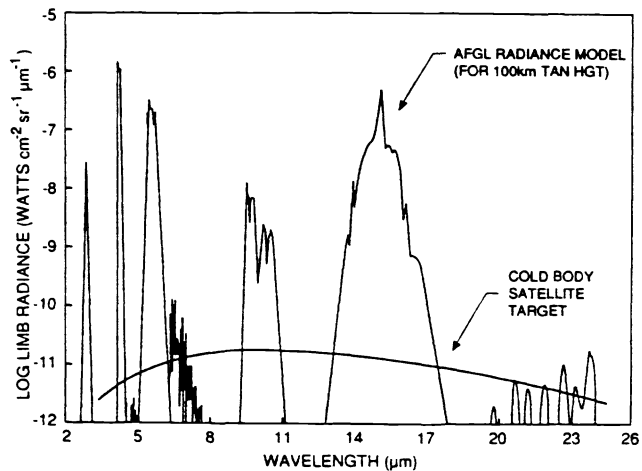


Figure 1. Air Force earthlimb model of atmospheric infrared emissions² compared with a theoretical 300° K 1m² blackbody target.

In addition, the auroral data will be used to validate and refine nuclear predictive codes.

3. SENSOR DESIGN

The primary CIRRIS 1A sensors are a high-resolution Michelson interferometer and a dual channel radiometer that share the common collecting optics of a high off-axis-rejection 0.3-m telescope. The optics, detectors, and preamplifiers are cooled with helium to temperatures of 12 K to maximize the instrument sensitivity to faint infrared sources. Coaligned on the outside of the telescope heat exchanger are two photometers, two low-light level television (LLTV) cameras, a 16-mm film camera celestial aspect sensor, and an infrared horizon sensor. The entire assembly is mounted on a two-axis-gimbal system to provide pointing and scanning capability. All of the sensor and housekeeping data are redundantly recorded on tape recorders for postflight reduction and analysis. The entire payload mass is 2045 kg. Figure 2 is an artist's drawing of the system, and Table 1 lists primary sensor specifications.

3.1 Telescope

The CIRRIS 1A primary sensors share the common collecting optics of a single high off-axis rejection telescope. Figure 3 shows the telescope, interferometer, and radiometer configuration. The telescope has a 30.48-cm diameter, D-shaped aperture with an image quality of 0.5 mr on axis, optical efficiency of 60%, and an out-of-field-of-view rejection of 1×10^{-10} at 2.5 degrees.

TABLE 1. CIRRIS 1A SENSOR SPECIFICATIONS

PARAMETER	INTERFEROMETER	RADIOMETER
Detectors	5-element IBC FPA	9-element Si:As FPA 5-element Si:Bi FPA
Optical Filters	8 selectable	7 selectable, 1 fixed
Noise Equivalent Spectral Radiance (NESR)	$3.7 \times 10^{-14} \text{ W cm}^{-2} \text{ sr}^{-1} \text{ cm}^{-1}$ at 700 cm^{-1}	-
Noise Equivalent Radiance (NER)	-	$7 \times 10^{-11} \text{ W cm}^{-2} \text{ sr}^{-1}$
Dynamic Range	A to D - 6.5536×10^4 Feedback resistor difference between channel 5 and other channels - 3×10^2 Electronic gain - 1×10^2 3 bias levels - 3×10^1 Ratio of det areas- 1.597×10^1 TOTAL - 9.42×10^{11}	A to D - 6.5536×10^4 Feedback resistor difference - 1×10^0 Electronic gain - 1×10^2 3 bias levels - 1×10^2 Ratio of det areas- 2.4×10^1 TOTAL - 1.57×10^{10}
Field of View	$.93^\circ \times 1.5^\circ$	$1.2^\circ \times 0.1^\circ$
Aperture	161 cm^2	182 cm^2
Chopper	-	Tuned fork at 84.6 Hz

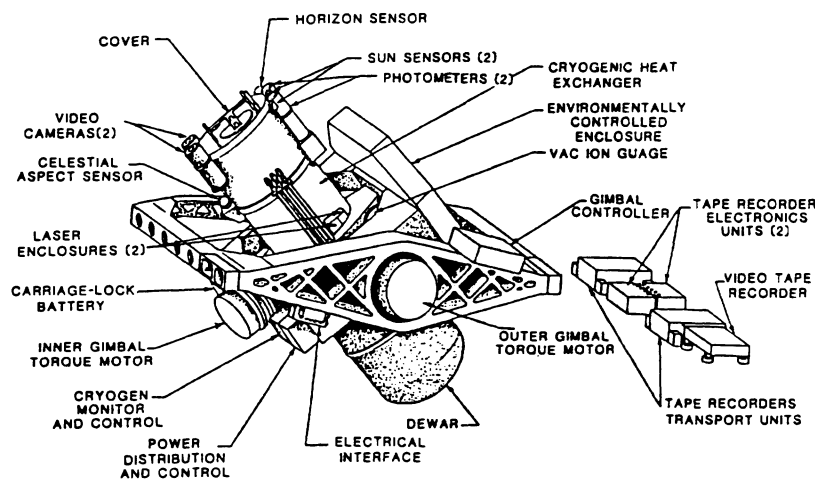


Figure 2. Component Layout of the CIRRIS 1A payload.

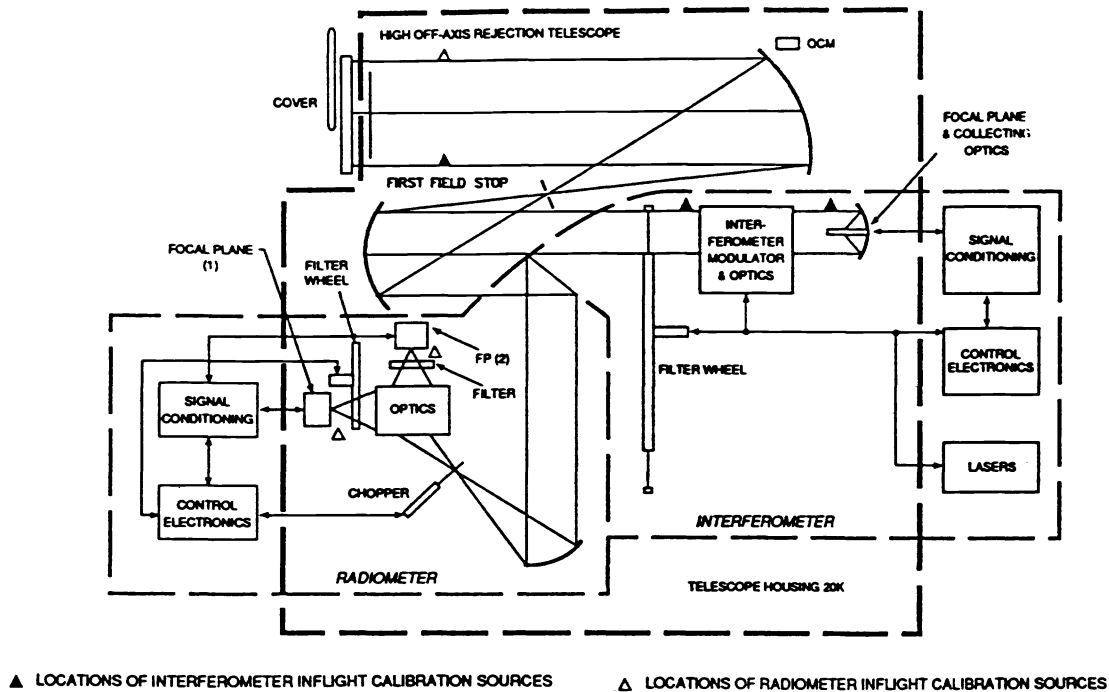


Figure 3. CIRRIS 1A telescope, interferometer, and radiometer configuration.

3.2 Primary Sensors

3.2.1 Interferometer

The Michelson interferometer is a flex pivot design with three selectable scan lengths that provide spectral resolutions of 1, 4, and 8 cm^{-1} with moving mirror scan times of 9.7, 2.7, and 1.5 sec, respectively. The spectral sensitivity of the interferometer is 4000 - 400 cm^{-1} . The interferometer focal plane array (FPA) is an impurity band conduction (IBC) type silicon doped arsenic (Si:As) with five detector elements designed for various measurement scenarios and resolutions. Figure 4 shows the CIRRIS 1A interferometer focal plane configuration. The focal plane optics are Ritchey-Chretien $f/1.6$. An 8-element filter wheel is used to reduce photon noise in selected band passes, shown in Figure 5, by minimizing out-of-band radiation. Built into the interferometer is an auto-alignment mechanism that allows on-orbit alignment of the interferometer optics should they become misaligned from forces encountered during launch.

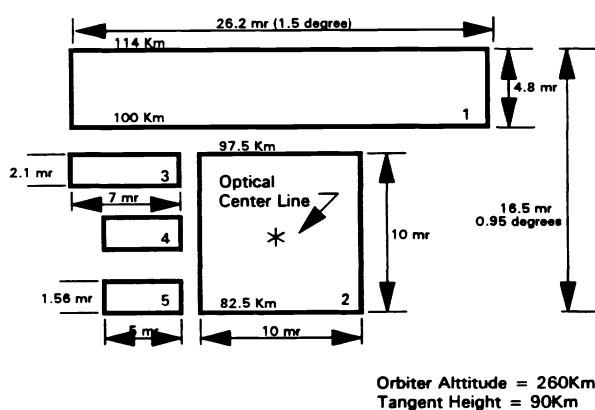


Figure 4. Interferometer focal plane configuration showing angular subtense and point spatial extent.

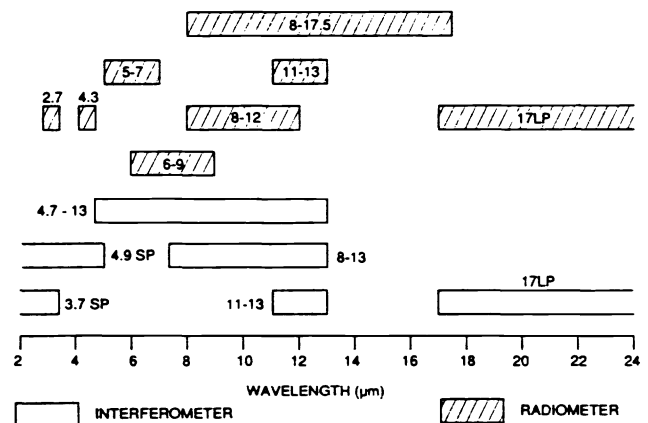


Figure 5. Interferometer and radiometer filter band passes.

3.2.2 Radiometer

The CIRRIS 1A radiometer is a two-channel radiometer with a dichroic beamsplitter. The radiometer focal plane arrays consist of a 9-element Si:As array and a 5-element bismuth-doped silicon (Si:Bi) array. Figure 6 shows the configuration of these focal planes. Both of the radiometer focal planes are coaligned with the interferometer focal plane. The 9-element FPA is located behind an eight-position filter wheel, while the 5-element FPA is housed behind a 2.95- μm fixed filter. The radiometer filter band passes are shown in Figure 5. The fixed filter acts as a constant reference channel for comparison with the 8 selectable band pass filters. This two-channel design allows simultaneous radiometric measurements in two wavelength regions, i.e., auroral emissions at 2.95 μm . A combination of detector sizes, bias levels, and signal conditioning electronics makes the radiometer sensitive over a wide dynamic range; it is capable of measuring zodiacal light, earthlimb emissions, and hard-earth emissions.

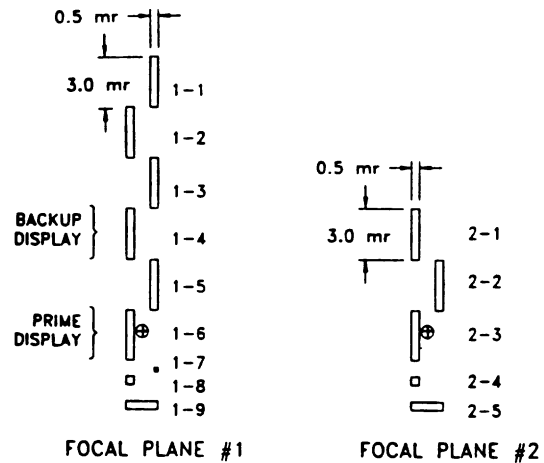


Figure 6. Radiometer focal plane configuration.

3.3 Ancillary Instruments

All of the CIRRIS 1A ancillary instruments were coaligned with the primary sensor line of sight. Figure 7 shows the field of views of all the sensors.

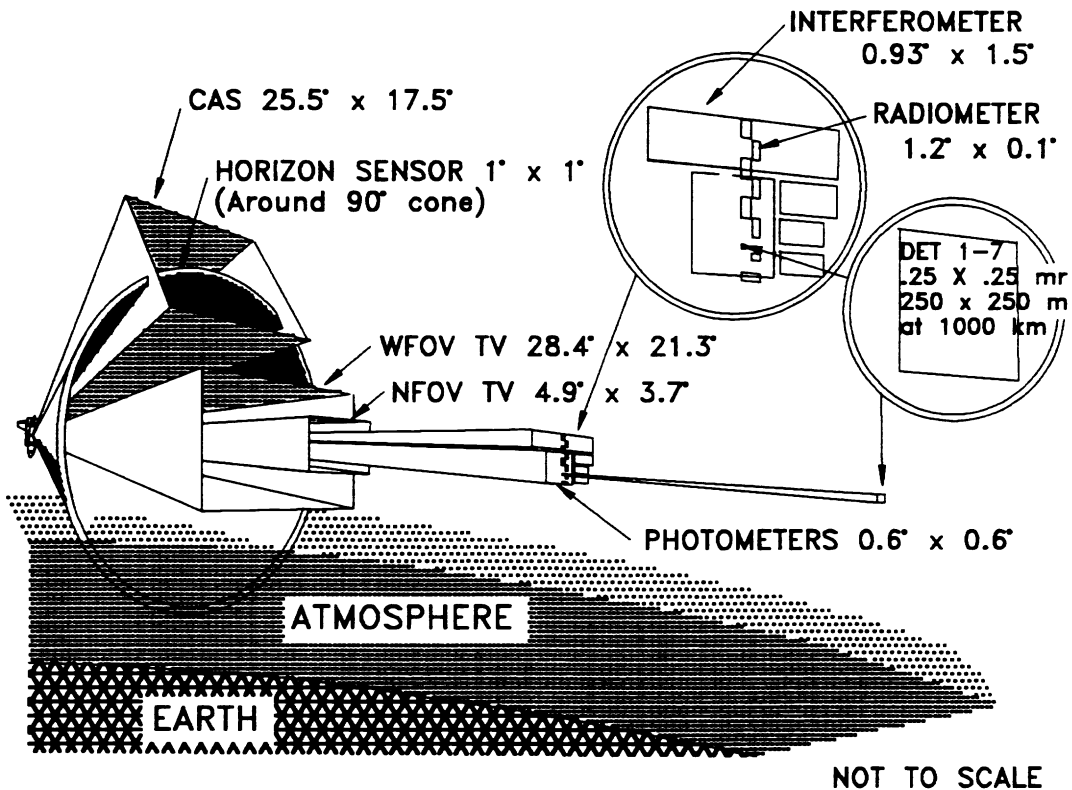


Figure 7. Fields of view for CIRRIS 1A infrared and ancillary sensors.

3.3.1 Photometers

The externally mounted photometers are band pass filtered to detect visible and ultraviolet radiation at 5577Å and 3914Å. The 5577Å photometer acts as both an auroral and airglow monitor for atomic oxygen $^1\text{S-}^1\text{D}$ emission while the 3914Å channel monitors the nitrogen ion, N_2^+ (0-0), band that serves as a monitor for electron deposition into the upper atmosphere, such as in an auroral event. Each photometer incorporates a sun sensor that automatically shuts down the photometer when the sun enters the 40° field of view of the sun sensor, the restricted field of view for the infrared telescope.

3.3.2 Low-Light-Level Televisions (LLTV)

Two LLTVs are coaligned with the telescope to assist the shuttle crew members in pointing the CIRRIS 1A instrument at visible targets of interest. The acquisition camera has a wide-angle field of view (28.4° X 21.3°) and the pointing camera has a narrow field of view (4.9° X 3.7°), slightly larger than the total field of view of the interferometer and radiometer. During flight operations the crew was able to select one of the camera outputs for display on the orbiter aft flight deck closed circuit television screens and used that display to point the sensor using a joystick controller.

3.3.3 Celestial Aspect Sensor (CAS)

The CAS is a 16-mm film camera mounted such that its field of view is 45 degrees from that of the telescope. In this orientation, it recorded the star field while CIRRIS 1A collected earthlimb data. Postflight data reduction of the film in conjunction with the orbiter ephemeris information is being used to determine where the instrument was pointing at a given time. The camera was also used to help analyze contamination by photographing sunlit particles in the vicinity of the shuttle cargo bay.

3.3.4 Horizon Sensor

The horizon sensor detects the displacement of the CIRRIS 1A instrument above the 40-km CO_2 layer. By sensing pitch and yaw angles relative to this emission source, the horizon sensor provided real time data on sensor pitch and yaw to the crew. The gimbal controller also received these data in certain scan modes, where it was important to maintain a constant pitch angle with respect to the horizon.

3.3.5 Pointing System

The pointing system is a two-axis system that rotates the CIRRIS 1A sensor in the orbiter pitch and roll planes in response to commands from either the CIRRIS 1A avionics, the orbiter aft flight deck command and monitor panel, or the crew-held joystick as various mission modes require. Main system elements include the gimbal frames proper, drive and brake elements, and control electronics. The gimbal proper consists of two nested structural frames. The outer frame is rigidly attached to the shuttle experiment support system (ESS) at four points. Suspended from the fore and aft beams of this outer frame is an inner frame that rotates about an axis parallel to the orbiter's roll axis, enabling the instrument to sweep through an angle of ± 38 degrees from top dead center in the roll plane. The CIRRIS 1A instrument itself is suspended in turn from the inner frame about an axis parallel to the orbiter's pitch axis through a sweep of +6 degrees (aft) to -24.5 degrees (forward) from top dead center in the pitch plane.

The gimbal controller directed and monitored all gimbal operations in response from the CIRRIS 1A avionics or commands from the aft flight deck. Two identical drive brake modules, responding to commands from the gimbal system controller, moved the sensor through various scan patterns. Each module contains, in addition to the driving torque motor, a 16-bit optical shaft encoder to provide position information, a tachometer to measure rotation rate, and a fail-safe brake.

4. FLIGHT OPERATIONS

CIRRIS 1A was launched on 28 April 1991 from Kennedy Space Center (KSC) on board the space shuttle Discovery (STS-39) into a 260-km circular orbit at an inclination of 57 degrees. The shuttle landed at KSC on 6 May 1991 after a very successful mission. SDL/USU, Phillips Laboratory, and other essential flight operations personnel were located at the Payload Operations Control Center (POCC) at Johnson Space Center (JSC) to assist the mission specialists. Although no downlink existed to acquire continuous real time data, flight operations personnel at JSC verbally obtained temperature and vacuum trending data, tape recorder hours used, and various other parameters from the mission specialists. This enabled the CIRRIS 1A scientists and engineers to closely follow instrument performance. Figure 8 is an example of a POCC trending graph.

Prior to flight, the CIRRIS 1A team developed an exhaustive set of experiment measurement plans to achieve the mission objectives. Over 55 complex measurement scenarios were devised to accommodate every foreseeable contingency. A subset of high priority measurements was developed from these scenarios. Flight operations personnel had the flexibility to reschedule the mission timeline, when necessary during flight, to optimize data acquisition.

The CIRRIS 1A on-orbit operations included vertical, horizontal, stare, and staircase scan modes of the earthlimb using various interferometer, radiometer, filter, and scan pattern combinations. Figure 9 shows these measurement scenarios. The orbiter orientation for most of the measurement blocks was a nosedown gravity gradient attitude, which provided a fairly stable pointing platform without the use of attitude control thrusters, which could cause irrecoverable damage to the sensor from deposition of contaminants onto the primary mirror. The mission specialists, using a command and monitor panel in the aft flight deck, initiated all measurement sequences. They tracked events such as aurora and targets of opportunity using the CIRRIS 1A manual pointing controller (joystick) while guided by imagery from the low-light-level televisions that were displayed on the aft flight deck closed circuit television system.

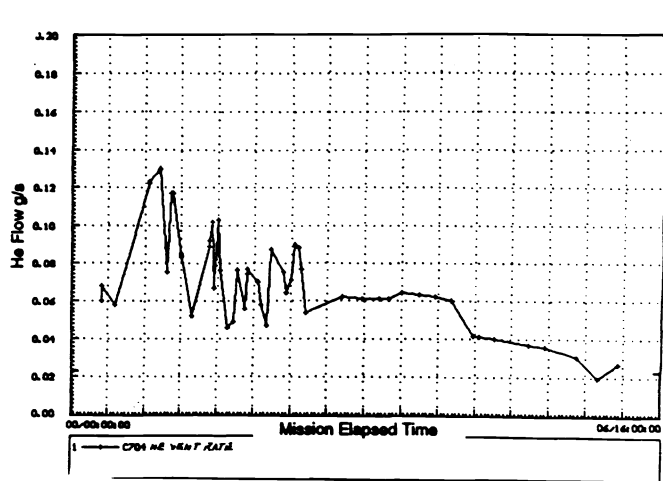


Figure 8. Example of POCC trending graph.

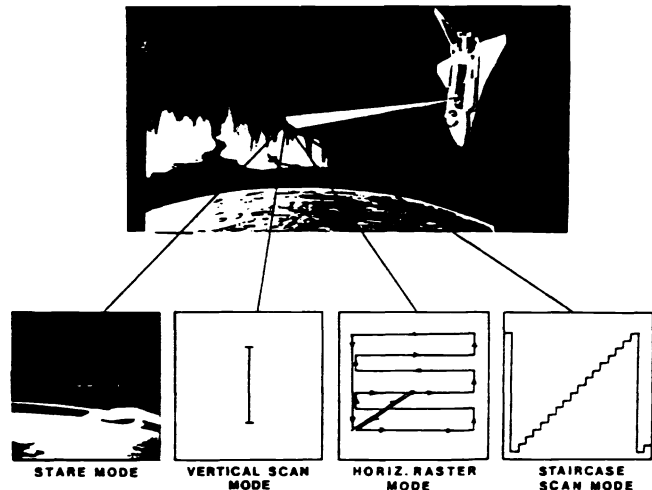


Figure 9. Typical CIRRIS 1A scan patterns.

To prevent contamination of the telescope's cryogenic surfaces, especially the primary mirror, cover-open measurements did not start until after approximately 24 hours on orbit. This allowed the gaseous and particulate contamination inherent with the space shuttle to outgas and disperse to acceptable levels. After performing initial health and status checks, the crew began the planned measurements.

Because auroral measurements were a high priority, the mission specialists maintained an auroral watch. Less than 24 hours into the flight, strong auroral activity was detected. Flight operations personnel replaced the scheduled flight blocks with auroral blocks at this time. Excellent data were obtained during these measurements, and the mission specialists did an excellent job pointing the instrument to optimize data takes. This strong auroral activity allowed CIRRIS 1A to achieve all of its auroral objectives.

Approximately 33 hours into the flight, CIRRIS 1A operations were extended through the next 24 hours because it appeared that the cryogen would run out earlier than predicted. Flight operations personnel then began replanning the mission timeline to optimize data acquisition. Several of the lower priority measurements were eliminated or only partially performed as a result of this replanning. This loss was insignificant, however, since most of the lower priority items were interwoven into the large number of data takes already performed. Virtually all of the top priority measurements were successfully performed during the mission.

The on-orbit ability of the flight crew to make technical judgments and to interact to select and operate very complex scientific instrumentation was of extreme value in executing the CIRRIS 1A experiment.

5. INSTRUMENT PERFORMANCE

All of the CIRRIS 1A instruments arrived on orbit in a fully functional condition and met or exceeded all specifications and requirements during the mission. The interferometer and radiometer functioned in nearly 140 different operational measurement modes and nearly 20 hours of prime data were collected and stored on the CIRRIS 1A tape recorder units. The interferometer arrived on orbit in proper alignment, indicating that all optical, mechanical, and electrical elements of the interferometer remained in position throughout the launch phase.

The ancillary instruments also operated successfully on orbit. The LLLTVs provided scenes ranging from celestial to hard earth views. The wide field-of-view (WFOV) camera reticle altitude settings correlated to the predicted altitudes of the aurora and air glow. The narrow field-of-view camera sensitivity appeared to be nominal and the autoranging capabilities worked as designed. Coalignment appeared to be closely correlated to the WFOV camera, as expected. The photometers experienced decreased responses during flight, but still provided useful data. Their outputs varied with differences in the observed brightness of the aurora, and in most cases the photometers' counts increased simultaneously, as desired. Post flight testing showed that the photometers were working properly, although at a decreased sensitivity. The celestial aspect sensor, horizon sensor, and data handling and recording equipment performed satisfactorily and as designed during flight. The pointing system performed satisfactorily and as designed. The most difficult operation involved pointing and tracking of resident space objects (RSOs).

The CIRRIS 1A cryogen system successfully cooled the optical elements through more than 24 hours of data acquisition. However, the predicted parasitic helium flow rate nearly doubled during periods of flight, and the dewar helium pressure increased. This resulted in an earlier than predicted cryogen run out, and necessitated rescheduling the flight operations timeline to assure that all CIRRIS 1A operations could be accomplished. With the amended timeline, all significant operations were completed, and the deviations in the cryogen system predictions did not affect the success of the mission.

6. FLIGHT DATA

Approximately 18 hours of airglow and auroral data were recorded on the CIRRIS 1A tape recorders during the mission. This includes about 150,000 interferometer spectral scans and 30 gigabytes of multispectral radiometer data. After flight, the flight data tapes were re-recorded onto optical disks in a 9-file format. The flight data are currently being analyzed by the computer aided system OPUS (Optical Physics User System), developed by Boston College.

Figures 10 through 14 are samples of preliminary flight data results from the CIRRIS 1A mission. Figure 10 shows the interferometer spectrum of earthlimb radiance in the nitric oxide (NO) fundamental band. The data also provided the first observation of ultra-hot Quiesen emissions in the dayglow regions. The NO spectrum in Figure 10 accurately follows the predicted models, and illustrates the high quality and resolution of the CIRRIS 1A flight data.

Figure 11 represents the first measurements of the far long-wave infrared (LWIR) window. Rotational water is the dominant emitter in this spectrum; hot OH is also present. In general, the CIRRIS 1A data indicate that diurnal variability is low in this window, and that the current SHARC model predicts the magnitude of the emission.

Because the radiance structure is limited to narrow bands, the far LWIR window may be the potentially cleanest window in which to observe a blackbody emitter.

Figure 12 shows sunlit-enhanced LWIR earthlimb spectra taken at a tangent height of approximately 80 km during dark and sunlit conditions. These spectra show that a lower amount of ozone exists during sunlit conditions, and that the CO₂ observed during sunlit conditions agrees with the SHARC model.

Figure 13 is a typical spectrum of the emissions observed in the 600 - 1450 cm⁻¹ wavelength region, showing the primary emitters. The data were taken at a 25-km tangent height. This spectral band represents the 8 - 12 μm atmospheric window through which the earth radiates a majority of its terrestrial radiation to space. Changes in absorption and emission in this region, due to changes in atmospheric constituents and their concentrations, have the highest potential to moderate the effectiveness of the earth's greenhouse response.

Figure 14 is a composite figure showing the 800-950 cm⁻¹ region of all of the spectra collected in one staircase mode. Overlapping altitudes are due to the overlap of detector foot prints on adjacent stair steps. The numbers by the spectra on the left hand side are the tangent heights. The emission bands of CFC-11, HNO₃, and CFC-12 are clearly evident at the lower tangent heights, and fade into the noise at higher altitudes.

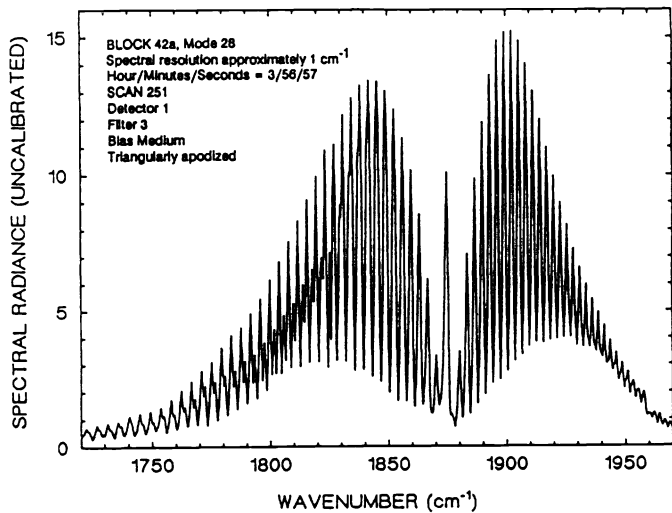


Figure 10. Earthlimb radiance in the nitric oxide fundamental band (CIRRIS 1A preliminary data).

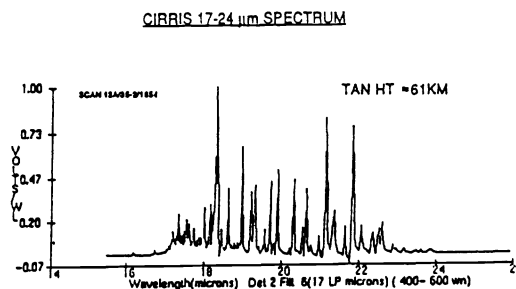


Figure 11. First measurements of far LWIR window (CIRRIS 1A preliminary data).

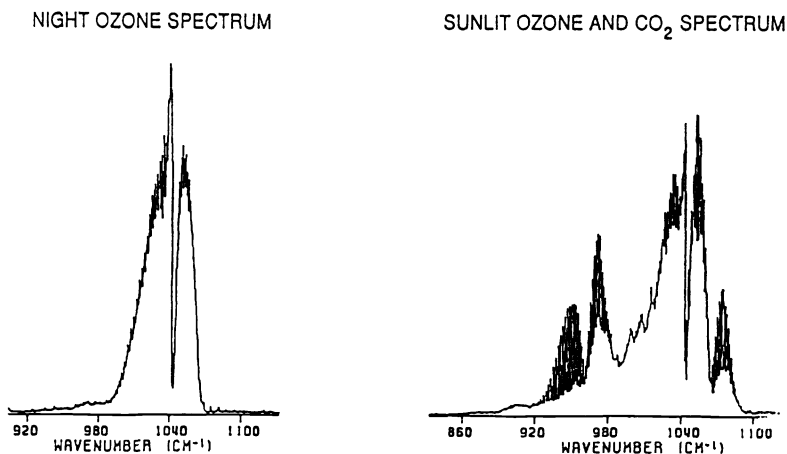


Figure 12. Sunlit enhanced LWIR earthlimb data (CIRRIS 1A preliminary data).

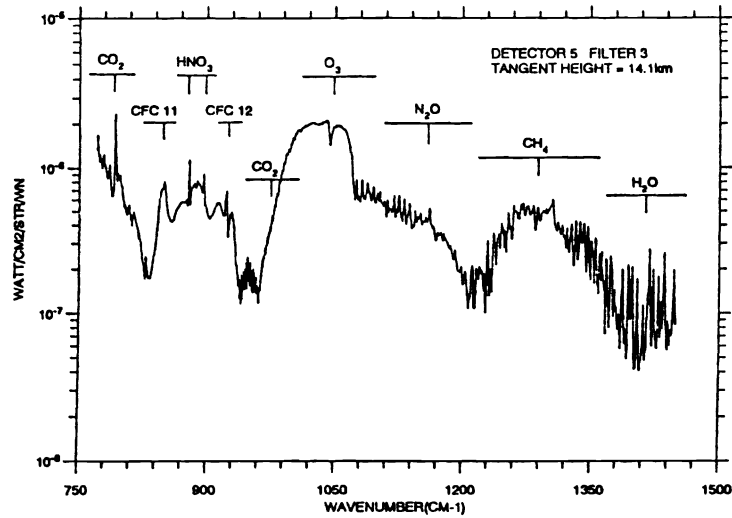


Figure 13. CIRRIS 1A interferometer greenhouse gas emission data (CIRRIS 1A preliminary data).

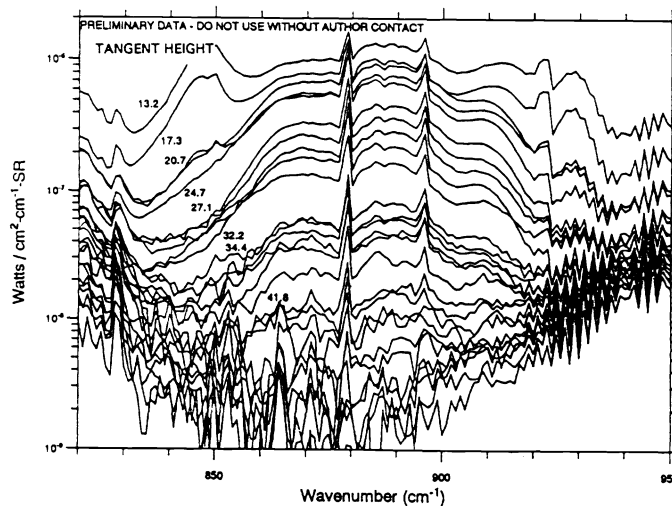


Figure 14. CIRRIS 1A spectra collected over one staircase mode (CIRRIS 1A preliminary data).

7. SUMMARY

The CIRRIS 1A atmospheric measurement experiment was designed to obtain simultaneous spectral and spatial infrared measurements on a variety of upper atmospheric phenomena. The instrument flew on board the shuttle Discovery from 28 April to 6 May 1991, and obtained over 18 hours of earthlimb, airglow, aurora, and target data. These data will provide a comprehensive update and validation of upper atmospheric models for both the scientific and military community. Results will contribute to the understanding of atmospheric infrared radiative mechanisms and to the design and operation of space defense systems.

Acknowledgments

CIRRIS 1A is a Strategic Defense Initiative experiment conducted by the Atmospheric Backgrounds Branch, Optical/Infrared Technology Division of the Geophysics Laboratory, U.S. Air Force Material Command. The primary contractor is the Space Dynamics Laboratory of Utah State University, along with the Space Data Corporation, Sensor Systems Group, and Boston College as subcontractors. Integration and flight operations support were provided by the Space Test Program Office of HQ Space Systems Division, the Aerospace Corporation, Lockheed Missiles & Space Company, NASA Johnson Space Center, and NASA Kennedy Space Center.

References

¹Jursa, A.S., "Handbook of Geophysics and the Space Environment," Air Force Geophysics Lab., Air Force Systems Command, U.S. Air Force, Hanscom AFB, MA, 1985, pp. 18-1-18-80.

²Degges, T.C., and Smith, H.J.P., "A High Altitude Infrared Radiance Model," AFGL-TR-0271, Air Force Geophysics Lab., Air Force Systems Command, U.S. Air Force, Hanscom AFB, MA 1977.

³Bartschi, B., J.C. Kemp, D.A. Burt, G.D. Allred, and L.J. Zollinger, "Applying an Interferometer Spectrometer Aboard the Space Shuttle with a Payload Specialist in the Control Loop," SPIE, Vol. 787, May, 1987.

⁴Ahmadjian, M., R.M. Nadile, J.O. Wise, and B. Bartschi, "CIRRIS 1A Space Shuttle Experiment," Journal of Spacecraft and Rockets, Vol. 27, No. 6, pp. 669-674, November and December 1990.